*The utilization of the kinetic and thermodynamic signatures of preclinical leads is proving pivotal in their triage and rational optimization towards clinical candidates with maximal **in vivo** efficacy devoid of adverse events.*

Target–drug interactions: first principles and their application to drug discovery

Sara Núñez[1], Jennifer Venhorst[1] and Chris G. Kruse

Abbott Healthcare Products, 1381 CP Weesp, The Netherlands

In this review, we begin by introducing the basic principles of kinetics and thermodynamics of target–drug binding within the context of drug discovery. In addition, we present a meta-analysis of the recent literature describing the kinetic and thermodynamic resolution of successful clinical candidates with diverse mechanisms of action. We finish by discussing the best practices in the triage and chemical optimization towards clinical candidates with maximal *in vivo* efficacy devoid of adverse events.

Sara Núñez studied organic chemistry at the University of Barcelona (Spain) and the University of London (UK). She received her Ph.D. in 2003 from the University of Manchester (UK), and thereafter did a postdoc in Biophysics at the Albert Einstein College of Medicine (USA). In 2005, she joined Solvay Pharmaceuticals (now Abbott Healthcare) in The Netherlands as a postdoctoral fellow; and in 2008, she was promoted to Sr. Computational Medicinal Chemist. At Abbott, she has supported the medicinal chemistry efforts for neuroscience drug discovery programs, from target discovery up to and including clinical proof of principle studies. She has supported more than 15 programs internationally, and was project manager of the D2-103 Top Institute Pharma innitiative.

Jennifer Venhorst obtained her MSc in Medicinal Chemistry *cum laude* from the Vrije Universiteit Amsterdam (VUA), The Netherlands in 1996. After working as a scientist at the Ludwig Institute for Cancer Research in Melbourne, Australia, she returned to the VUA in 1997 to obtain her Ph.D. in Molecular Toxicology and Computational Chemistry. Following a short post-doctoral period, she joined Solvay Pharmaceuticals (now Abbott Healthcare) in 2002. As Senior Computational Medicinal Chemist at Abbott, Jennifer has provided support for a wide range of international drug discovery programs related to Neuroscience and Women's Health indications. Her activities covered all stages of drug discovery, from target validation to clinical candidate selection. She additionally headed the global Center of Excellence for target-drug interactions.

Chris G. Kruse studied organic and medicinal chemistry at Leiden University, the Netherlands. He received his Ph.D. in 1978. His first job in industry was with Philips Forschungslabor in Germany. Thereafter he joined Solvay Pharmaceuticals (now Abbott Healthcare) in 1981. At Abbott, he has maintained several positions both in the medicinal chemistry and process research chemistry departments. He has also been responsible for the drug discovery efforts in the psychiatry area ranging from target discovery up to and including clinical proof of principle studies until 2007, leading to the discovery of more than 10 clinical candidates. His recent responsibility was head of medicinal chemistry for the 3 ex-Solvay research sites in France, Germany and The Netherlands. He is also professor of drug discovery sciences at the University of Amsterdam since 1997.

Introduction

A considerable portion of drug discovery focuses on the lead finding and optimization of ligands (drugs) by evaluating, among other properties, their affinity to the primary target [1]. Typically, large libraries are screened against the primary target at a high ligand concentration. Subsequently, affinity and/or efficacy thermodynamic equilibrium constants are derived for the most active primary hits by way of dose response determination, leading to a top-ranked list of chemical entities. In practice, the *in vitro* affinity of a ligand to the primary target is regarded as an acceptable surrogate of its *in vivo* efficacy. Yet, the attrition rates of promising leads for validated targets that meet primary *in vitro* pharmacodynamic (PD) criteria are considerable owing to their failure to meet *in vivo* end points [2]. This finding led the scientific community to realize that advancing compounds (ligands) based on their primary *in vitro* binding profile might be too simplistic a strategy. In effect, the exclusive use of steady-state metrics in the triage and advancement of best leads towards the clinic has become obsolete.

Kinetic signature of target–drug binding

Binding kinetics is concerned with the rate constant of ligand association (k_{on}) and ligand dissociation (k_{off}). The ratio of the dissociation to the association rate constants establishes the equilibrium dissociation metric of the ligand ($K_d = k_{off}/k_{on}$), which determines the fraction of receptor occupancy at specific ligand concentrations; K_d, k_{off} and k_{on} are intrinsic to the target–drug interaction in question.

Corresponding author:. Núñez, S. (nunez.sara@gmail.com)
[1] Both authors contributed equally to the studies presented.

There are two general binding mechanisms for a target–drug pair. In mechanism 1, the receptor (R) and ligand (L) combine to form a binary complex RL with association/dissociation rate constants k_1 (k_{on}) and k_2 (k_{off}), respectively (Eqn (1)):

$$R + L \underset{}{\overset{k_1}{\rightleftharpoons}} RL \tag{1}$$

In mechanism 2, the ligand encounters the receptor (R) in a conformational state that is suboptimally complementary to the ligand for binding. Subsequent to the initial encounter (RL), the receptor undergoes a conformational change to a more committed state (R*) where the new binary complex (R * L) has a more competent binding affinity than RL (Eqn (2)).

$$R + L \underset{k_2}{\overset{k_1}{\rightleftharpoons}} RL \underset{k_4}{\overset{k_3}{\rightleftharpoons}} R * L \tag{2}$$
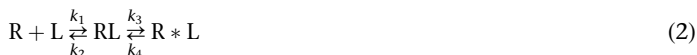
Two equilibrium dissociation constants are required to describe this so-called 'induced fit' mechanism. Hence, the value of k_{off} for mechanism 2 is not defined by a single microscopic rate constant. Instead, k_{off} entails an array of diverse rate constants associated with both RL and R * L, such that $k_{off} = k_2k_4/(k_2 + k_3 + k_4)$. In most instances, it is the reverse isomerization rate constant k_4 that is rate limiting with respect to R * L dissociation. This isomerization step adds significant potential for a more enduring partnership between the target and the ligand (Table 1). In fact, most ligands with resilient k_{on} and k_{off} rates are dictated by mechanism 2, in which a temporal isomerization (e.g. tautomerization) of the target (and/or ligand) to a novel state is most suitable for target–drug binding to occur [8,9].

At this point, it is important to highlight two common scenarios where a target and its ligand physically encounter each other in solution. The first is termed the 'closed system', where the total receptor and ligand concentrations are constant over time. In this scenario, the only change in concentration that takes place over time is the concentration of free and bound species as the system approaches equilibrium. Thereafter, the measurements of equilibrium dissociation constants are performed [5]. In this case, the target–drug complex lifetime is approximated by the equilibrium dissociation constant [1]. The second scenario is the open system, which is more relevant to physiological conditions. Here the receptor is typically kept at a fixed concentration whereas the ligand concentration is allowed to vary, mirroring factors such as metabolic clearance or diffusion through cellular compartments. Thus, the open system is characterized by continuous changes in the flux of ligand that is available for encounter with the receptor. Because the concentration of the ligand continuously changes in an open system, equilibrium measurements are not feasible.

Measuring kinetics

Optical biosensors are the most popular means of studying binding events, because they enable label-free, high-throughput binding measurements in real time. Kinetic characterization by way of surface plasmon resonance (SPR) is the most established method, although other equally valid methods have been reported [10]. In SPR, the protein of interest is immobilized on a coated gold film surface, which is then exposed to the analyte or drug in flow (Fig. 1) [11]. Analyte binding induces a change in the refractive index on the sensor surface. This change is linear to the number of molecules bound, making SPR a quantitative technique.

Typical SPR sensorgrams, where the change in refractive index due to analyte binding is monitored as a function of time, are shown in Fig. 2. The rate constants k_{on} and k_{off} are estimated by regression of the association and dissociation gradients at different ligand concentrations. For mechanism 1, both steady-state equilibrium and kinetic phase characterization can be performed with sensorgrams. In particular, the kinetic binding constant can simply be derived by $K_d = k_{off}/k_{on}$. The steady-state constant can be determined by plotting the response at equilibrium against the ligand concentration, where the K_d equals 50% of the maximum response. For mechanism 2, SPR appears to be less suited because the post-binding conformational change does not affect the signal of the SPR apparatus based on a change in mass. This is because the ligand remains bound. Moreover, induced fit effects are expected to occur on a much faster time scale (nano- to millisecond) than SPR can measure [12]. Post-binding conformational changes have nevertheless been reported for drugs using SPR (e.g. the acetylcholine binding protein [13]); whether these observations are artifacts remains to be seen.

Biosensor-based methods are not free of experimental limitations. First, the SPR signal is highly sensitive to temperature variations and changes in bulk solvent. Measurements need to be performed under highly stable conditions and with a fully dissolved ligand. Furthermore, the effect of mass-transport limitation (MTL), where the association rate is faster than the ligand diffusion rate from the bulk solvent into the biosensor surface, is often observed [14]. This results in a lower ligand concentration in the vicinity of the sensor surface when compared with the bulk, which leads to an underestimated association rate. Moreover, because a fast k_{on} predisposes to the ligand rebinding event, a 'retention zone' can be formed, and this leads to an underestimation of k_{off}. Thus both k_{on} and k_{off} might appear lower in magnitude owing to the MTL effect. It has been established that the upper limit for k_{on} determination by SPR is $10^6\,M^{-1}\,s^{-1}$, whereas the fastest k_{off} that can be accurately measured is approximately $10^{-1}\,s^{-1}$ [15]. Another factor that might result in a misleading kinetic readout is surface binding site heterogeneity [14].

A closer look at the association/dissociation rates

The association rate of a target–drug complex is determined by both the magnitude of k_{on} and the ligand concentration at the receptor site. As mentioned above, the ligand concentration can easily vary under physiological conditions (i.e. an open system) as a result of factors, such as absorption, clearance or promiscuous binding to alternative partners. Although the k_{on} value varies among target–drug pairs, this rate constant is ultimately limited by physicochemical steps, such as the diffusion rate of the binding partners or desolvation penalties. Diffusion coefficients depend acutely on the physicochemical properties of the binding partners. Hence, within a series of closely related chemical analogs, the diffusion coefficients are expected to be nearly identical, leading to comparable k_{on} rates [16]. Accordingly, drugs tend to have intrinsically large on-rate constants (10^3–$10^9\,M^{-1}\,s^{-1}$) because these are merely limited by pharmacokinetic (PK) processes. Also, fast association kinetics can favor rebinding (or reassociation) between the target and the ligand, leading to a higher target occupancy and, thus, *in vivo* pharmacological action [6,17].

TABLE 1

Compounds with fast, slow or irreversible dissociative half-lives

Compound	Mechanism of action	Half-life ($t_{1/2}$s)	Refs.
Deoxyconformycin	Adenosine deaminase	40 hour	[3]
Candesartan	AT1 receptor	2–3 hour	[4]
Olmesartan	AT1 receptor	72 min	[4]
Telmisartan	AT1 receptor	1.3 hour	[5]
Formestane	Aromatase	Mechanism based	[4]
Maraviroc	C–C Chemokine receptor 5	136 hour	[6]
Rofecoxib	Cyclooxygenase-2	9 hour	[3]
Aspirin	Cyclooxygenase	Irreversible	[4]
Celecoxib	Cyclooxygenase-2	Irreversible	[4]
Trimethoprim	Dihydrofolate reductase	8 min	[3]
Methotrexate	Dihydrofolate reductase	35 min	[3]
Saxagliptin	Dipeptyl peptidase IV	212 min	[5]
Haloperidol	Dopamine 2 receptor	40 min	[5]
Clozapine	Dopamine 2 receptor	0.5 min	[5]
Quetiapine	Dopamine 2 receptor	0.3 min	[5]
Lapatinib	Epidermal growth factor receptor	5 hour	[4]
Vigatatrin	GABA transaminase	Irreversible	[4]
Sufugolix	Gonadotropin-releasing hormone receptor	2.7 hour	[5]
NBI 42902	Gonadotropin-releasing hormone receptor	4.3 hour	[5]
Procarbazine	Guanine alkyltransferase	Irreversible	[4]
Omeprazole	H^+K^+ ATPase	Irreversible	[4]
Lansoprazole	H^+K^+ ATPase	Irreversible	[4]
Desloratadine	Histamine 1 receptor	>8.7 hour	[6]
GSK1004723	Histamine 1 receptor	5.8 hour	[6]
Darunavir	HIV-1 protease	>235 hour	[5]
Nelfinavir	HIV-1 protease	0.8 hour	[5]
Lopinavir	HIV-1 protease	1.2 hour	[5]
Compactin	HMG-CoA reductase	15 min	[3]
Geldanamycin	Heat shock protein 90	4.6 hour	[3]
Amlodipine	L-type calcium channel	77 min	[4]
Selegiline	Monoamine oxidase	Irreversible	[4]
Tranylcypromine	Monoamine oxidase	Irreversible	[4]
Tiotropium	Muscarinic M3 receptor	7.7 hour	[6]
Ipratropium	Muscarinic M3 receptor	0.16 hour	[6]
Aprepitant	Neurokinin 1 receptor	3.6 hour	[6]
Orlistat	Pancreatic lipase	Irreversible	[4]
Immucillin	PNP	8 min	[7]
DADMe-ImmH	PNP	20 min	[7]
DADMe-ImmG	PNP	2 hour	[7]
Finasteride	Steroid 5α-reductase	Mechanism based	[4]
Melagatran	Thrombin	36 s	[5]
Argatroban	Thrombin	2 s	[5]
Lepirudin	Thrombin	11 hour	[5]
Oseltamivir	Viral neuroaminidase	33–60 min	[4]
Allopurinol	Xanthine oxidase	5 hour	[3]
Buprenorphine	μ-Opioid receptor	166 min	[4]
Alvimopan	μ-Opioid receptor	30–44 min	[6]
N-Methylnaloxone	μ-Opioid receptor	0.46 min	[6]

TABLE 1 (*Continued*)

Compound	Mechanism of action	Half-life ($t_{1/2}$s)	Refs.
Clavulanate	β-Lactamase	Irreversible	[4]
Sulbactam	β-Lactamase	Irreversible	[4]
Tazobactam	β-Lactamase	Irreversible	[4]

By contrast, the dissociation rate is entirely dependent on the intermolecular complementarity within the bimolecular complex. The dissociation rate for a binary complex is first-order and, hence, independent of the 'unbound' ligand concentration gradient. Typical k_{off} values range from 10^{-6} to $1\ s^{-1}$ [18]. In the context of this review, the residence time is defined as the reciprocal of the dissociation rate constant for the target–drug complex. The residence time of a ligand on its target has been interpreted as the difference in free energy between the ground and transition states of the reaction co-ordinate [7]. Residence times of substrates bound to an enzyme are, in general, relatively short [19]. By contrast, enzymatic inhibitors with binding affinities in the nanomolar range present longer residence times and, therefore, sustained inhibitory effects (Table 1).

Association and dissociation rate constants are not intrinsically related to one another, but they are individually correlated with structural features of the compounds. The kinetic profile of structurally different compounds can consequently reveal features and aspects of compound–target interactions and aid optimization. The potential to ameliorate off-target toxicities with such ligands is equally important; this is explained below [20].

In most physiological situations, the duration of the biological effect produced by a target–drug complex is directly related to the lifetime of the binary complex; the longer the ligand is in residence at its receptor, the longer the biological effect lasts [1,21]. In essence, given a comparable K_d, the factor that differentiates ligands in terms of efficacy is primarily determined by the concentration-independent k_{off} constant to the primary target. Thus, the thermodynamic equilibrium constant of a ligand does not necessarily define the efficacy and duration of biological action; rather, it is the lifetime of the binary receptor–ligand complex that largely dictates the effect in the cellular context. Incidentally, k_{off} usually finds better correlation with K_i than does its counterpart k_{on} [3,5,16,22].

When the residence time of the biological complex is long, a significant level of receptor occupancy (and pharmacological efficacy) can be sustained, even when the systemic level of ligand has diminished significantly [5,23]. This has been demonstrated with various PK/PD simulations where the target occupancy of rapidly reversible ligands is entirely dependent on the ligand concentration at the target vicinity, which is in turn determined by its PK profile [7]. As such, ligands with half-lives ($t_{1/2}$) ≤ 1 hour precipi-
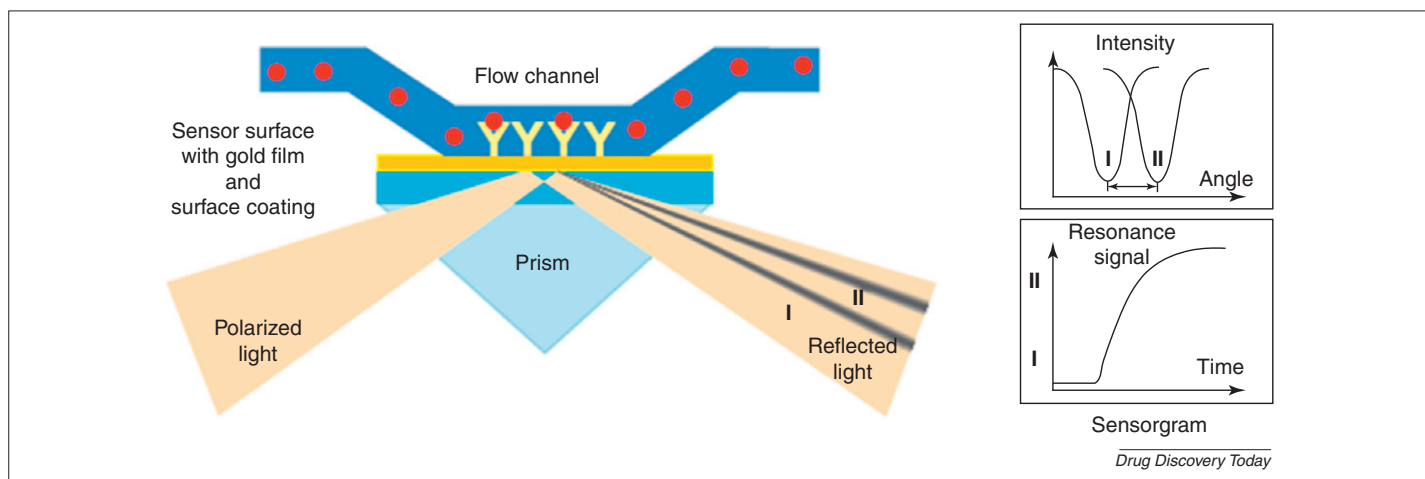

FIGURE 1

Basic configuration of a surface plasmon resonance (SPR) sensor. It consists of a prism mounted on a sensor chip with a thin gold film. The surface of the gold film on the side opposite the prism is coated and contains the immobilized target protein. The latter is exposed to the drug via a microfluidic flow channel. In essence, SPR makes use of the excitability of oscillating electrons at the metal film surface by light. When the quantum energy carried by light photons exactly equals the quantum energy level of the metal electrons, a plasmon is created. This is a group of excited electrons that behave as a single electrical entity. Under the conditions where incident light energy is absorbed and plasmons are created (i.e. attenuated total reflection), a dip in the intensity of reflected light is observed. The wavelength at which this occurs is termed the 'plasmon resonance wavelength'. The plasmon created generates an electrical field known as an evanescent field, on both sides of the metal surface. This field decays exponentially, the strongest being at the metal surface with a limited range of approximately 300 nm. SPR instrumentation exploits a unique feature of this plasmon field: any change in the chemical composition of the environment within the range of the evanescent field causes a change in the conditions at which light couples with the plasmon. This includes biomolecular interactions occurring at the sensor surface impacting the refractive index within the evanescent wave. The resulting shift in the wavelength of light, which is absorbed rather than reflected, can be measured as a change in resonance angle or resonance wavelength. The magnitude of the shift is quantitatively related to the magnitude of the chemical change. SPR instrumentation exploits exactly this dependency of the SPR signal on the chemical environment of the metal film carrying immobilized ligand exposed to potential binding partners.
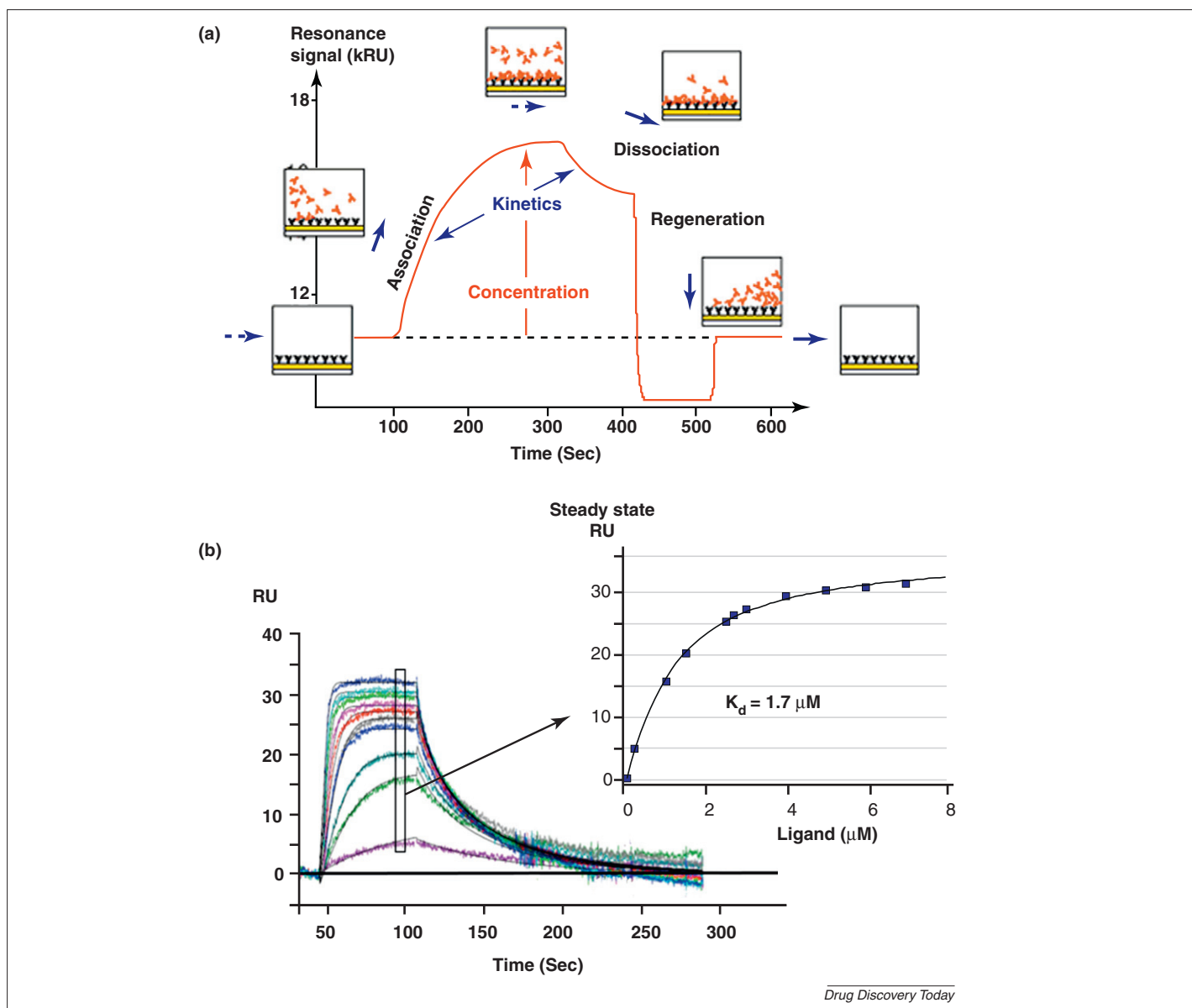Reproduced, with permission, from General Electric.

FIGURE 2

(a) A typical surface plasmon resonance (SPR) sensorgram. During sample injection, the drug binds to the surface-attached protein, resulting in an increase in signal. When the pulse of drug continues long enough, steady state is reached, as illustrated in the sensorgram as a flattening of the response. At the end of the injection, the sample is replaced by a continuous flow of buffer, and the corresponding decrease in signal reflects dissociation of the drug from the surface-bound complex. In this example, the response is expressed as arbitrary response units (RU). Reproduced, with permission, from General Electric. **(b)** By plotting the response units (RU) at equilibrium against the ligand concentration, the K_d can be derived: the K_d is equal to the ligand concentration at which the half maximal response is reached.

tate a prompt decay in target occupancy, whereas the percentage of target occupancy is longer for ligands with $t_{1/2} > 1$ hour. In essence, it is not the $t_{1/2}$ itself but rather the k_{off} and $t_{1/2}$ window, which determines whether the binding occupancy of a quasi-irreversible ligand will uphold that of the readily reversible one.

Finally, it has been suggested that 'kinetic selectivity' could provide a more informative metric for the therapeutic window. A drug that displays long residence time at its primary target and short residence times at collateral receptors will display a higher degree of target selectivity over the course of dosing. This will probably translate into a safer toxicological profile. Thus, the shorter the duration of the promiscuous residence at alternative partners, the safer the profile of the drug.

Long or short residence time?

Compounds exhibiting comparable target binding affinities do not necessarily have similar association and dissociation rates. By resolving their kinetic endowment, a differentiation among otherwise indistinguishable compounds can be made to steer compound prioritization and optimization. Whether to aim for, or shun, long residence times is a crucial consideration in early-phase discovery, because a long residence time can have both beneficial and detrimental outcomes. As such, two general approaches exist towards extreme target residence times. The first subscribes to the notion that longer ligand residence times confer enduring PD effects that outlast opposing PK factors. At the other extreme, it has been postulated that ligands with elusive residence times are
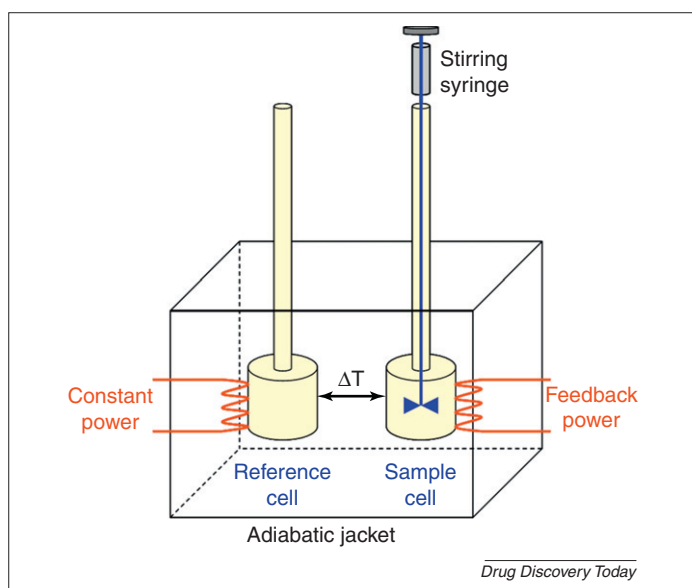
FIGURE 3

Basic configuration of an isothermal titration calorimetry (ITC) instrument. A pair of identical cells is located within an adiabatic jacket. Both the reference and sample cells contain identical buffer system, and the latter also contains the protein of interest. A constant power is applied to the reference cell to maintain a set temperature. The power applied to the sample cell (feedback power) is variable and equal to the power needed to maintain a constant temperature difference between the reference and sample cell. When a precise amount of ligand is titrated to the sample cell via the syringe, the heat evolved or absorbed owing to binding is reflected as a change in the feedback power. This differential power is proportional to the temperature differences between the reference and sample cell. Exothermic and endothermic interactions are characterized by negative and positive change in feedback power, respectively.
Adapted from [49].

desirable because they represent a good compromise between efficacy and mechanism-based toxicity [4]. Various examples are presented herein, demonstrating the kinetic preference for a diverse mechanism of action (MoA).

Short residence time
For pharmacological mechanisms requiring the endogenous ligand to perform routine physiological functions, a fast-binding exogenous ligand displaying short-lived intervention might be advisable.

Ion channel antagonism
A N-methyl-D-aspartate (NMDA) receptor antagonist is currently a first-line treatment for moderate and advanced Alzheimer's disease. It is a low-affinity, open channel blocker, which swiftly dissociates from the receptor. This enables the latter to return quickly to the resting state [24]. By contrast, the NMDA receptor antagonist ketamine and MK-801 block the channel with high affinity and slow dissociation rates. This results in mechanism-based adverse events and limits their clinical use.

Dopamine receptor antagonism
Dopamine-2 receptor antagonists (typical antipsychotics) are a first-line treatment in psychosis. However, because they often have adverse events [25,26], the use of atypical antipsychotics,

such as risperidone, has increased owing to their minimal risk of adverse effects. It has been proposed that the factor that can best account for atypicality is the faster dissociation rate from the dopamine-2 receptor. Rapid and competitive k_{off} rates are needed to prevent mechanism-based toxicity for dopamine-2 receptor antagonists [26].

Cyclooxygenase inhibition
Ibuprofen and naproxen are cyclooxygenase inhibitors that are used as anti-inflammatory agents; they differentiate from their analog acetylsalicylic acid (aspirin) by their rapid reversible inhibition. The irreversible binding profile of aspirin translates into long-lasting inhibitory effects, which platelets cannot overcome, thereby increasing the risk of bleeding events [27].

Immune response
Slow dissociation of ligands from their target receptors is often associated with a ligand-induced receptor conformational change that forces the compound into a conformation optimized for favorable interactions [20]. A ligand with a long residence time on such a receptor increases the duration of antigen presentation, and, therefore, might increase the chance of an immune response [28].

Long residence time
For therapies requiring enduring target occupancy, quasi-irreversible binding might be the most appropriate strategy. This is often termed 'insurmountable antagonism', where the ligand antagonizes the target function in a semi-irreversible manner [29]. The efficacy of ligands with 'ultimate physiological inhibition' is eventually overcome by the resynthesis of new target molecules [30]. The dosing interval required for effective ligand action in this case is therefore governed by this occurrence. In general, ligands with long residence time represent a majority and are considered to be of higher biological efficiency than are ligands with short residence time [1].

Angiotensin II type 1 antagonism
An example of a ligand with an exceptional dissociation rate constant is the angiotensin II type 1 (AT1) receptor antagonist candesartan, which differentiates from the 'surmountable' AT1 receptor antagonist losartan [31,32]. Although the underlying mechanism of the unsurmountability of candesartan is not yet completely understood, *in vitro* binding studies suggest that its long dissociative half-life relates to a two-step receptor isomerization. The slow k_{off} rate of candesartan has been attributed to its enhanced long-lasting blood pressure lowering effects *in vivo*, which have been reported to persist even after candesartan plasma concentration has become undetectable.

Trypsin inhibition
Vincent *et al.* measured the association and dissociation rate constants for several trypsin inhibitors [33]. Among different proteinase–inhibitor combinations, the association rate constants varied only 55-fold, from 10^4 to 10^6 M^{-1} s^{-1}. By contrast, the k_{off} values spanned a 10^5-fold range, corresponding to residence times from 22 min to 6 months. Thus, overall complex lifetime was almost exclusively determined by their residence times and

appeared to be an important factor in inhibition specificity for these systems.

HIV inhibition

Darunavir is the most recently Food and Drug Administration (FDA)-approved HIV protease inhibitor. It differentiates itself from its protease inhibitor analogs by an extremely long enzyme–inhibitor residence time. Importantly, the authors of the study linked this property to the highly potent antiviral activity of darunavir and the high genetic barrier to the development of resistance [34,35]. In another study with a panel of human and mouse antibodies specific to the V3 loop of the HIV-1 envelop glycoprotein gp20, VanCott et al. illustrated, that the variation in k_{on} across the antibody panel was only fourfold, whereas the values for k_{off} varied more than 100-fold [36]. The authors concluded that k_{off} correlated well with cellular potency, whereas no correlation was found between k_{on} and cellular potency.

Epidermal growth factor receptor inhibition

Wood and co-workers provided experimental evidence for the extended duration of cellular efficacy that can be achieved with inhibitors of the epidermal growth factor receptor (EGFR) tyrosine kinase receptor, which have long residence times [37].

Purine nucleoside phosphorylase inhibition

Genetic deficiency of human purine nucleoside phosphorylase (PNP) causes T-cell immunodeficiencies. DADMe-ImmG(H), a second-generation transition-state inhibitor, achieves greater in vivo efficacy than the first-generation analogs (ImmH). Lewandowicz et al. attribute this enhanced biological efficacy to the ultimate physiological inhibition of DADMe-ImmG(H), where the recovery of PNP enzymatic activity occurs primarily by resynthesis of new target molecules [30].

Ion channel agonism

In the cases where receptor desensitization represents an efficacy liability, repetitive ligand binding (i.e. fast k_{on} and k_{off} rates) could be detrimental. Examples are the nicotinic α7 receptor, and the γ-aminobutyric acid (GABA) receptor, for which partial agonism or even positive allosteric modulator (PAM) might prove a better approach to activate the ion channel.

In summary, the traditional drug discovery dogma that strives for affinity improvement might benefit from some level of kinetic input. The preference for long or short residence time is highly dependent on the MoA and the relevant pharmacological context. Making any statement on this aspect might not be possible at an early stage of drug discovery for a novel MoA. Thus, kinetic interrogation of the MoA with pharmacological tools spanning a range of residence times should be initiated as early as the target validation stage and maintained throughout all discovery phases. Lastly, a k_{off} selectivity window against secondary targets is advisable to avoid off-target adverse events. All these considerations warrant kinetic studies for the identification of clinical candidates with optimal in vivo efficacy devoid of mechanism-based toxicity.

Thermodynamic signature of target–drug binding

Binding thermodynamics provides a comprehensive view of the various types of molecular force that drive binding. These encompass the target and ligand desolvation, the restriction of the protein and ligand conformational freedom, among other factors. Most medicinal chemistry strategies gravitate towards optimization of ΔG, the Gibbs free binding energy. ΔG is the sum of two energetic terms, the enthalpy change (ΔH) and the entropy change (ΔS), such that $\Delta G = \Delta H - T\Delta S$. The equilibrium dissociation constant is dictated by the Gibbs energy of binding, $K_d = e^{-\Delta G/RT}$, where R is the universal gas constant and T is the absolute temperature. To achieve extremely high binding affinity a change in both binding enthalpy and entropy is required to contribute constructively [38–41]. Although the simultaneous optimization of enthalpy and entropy is the clear goal, medicinal chemists often find this objective is challenging to achieve. Rational enthalpic optimization is notoriously difficult and, if an enthalpic improvement is actually achieved, it is often not reflected in better affinity, because the enthalpy gain is compensated by an entropy loss. This is often described as enthalpy–entropy compensation [42]. In this context, numerous attempts have been made to measure the (de)solvation contributions; although there might not be many experimental approaches, several significant advances are being made computationally [43–47]. Thus, the benefits of using the individual thermodynamic binding terms in drug discovery are becoming more appreciated [48].

Measuring thermodynamics

Isothermal titration calorimetry (ITC) measures the binding enthalpy change by detecting the heat absorbed or released along the binding reaction co-ordinate (Figs. 4). The raw data generated by the instrument are converted to a binding isotherm, enabling direct or indirect extraction of the thermodynamic parameters, the stoichiometry n and K_a ($1/K_d$), (Fig. 3). To determine all parameters precisely, the curve needs to be sufficiently sigmoidal [50]; this shape is governed by K_a and the concentration of binding sites (i.e. the product of n and the protein concentration $[M]_t$). This dependency is often referred as the Wiseman c-parameter ($c = n[M]_t K_a$), which optimally has a value between 10 and 100.

ITC is a widespread technique that demands minimal method development; however, there are several limitations to its application, namely for very low or high potency ligands and entropy-driven ligands. In addition, a recent study highlights the significant variability in inter-lab ITC experiments [51]. With regards to low-affinity ligands, a borderline c-value and solubility limitations might hamper the derivation of thermodynamic data. However, parameter determination might still be possible under certain conditions [50] or by performing competition studies [52]. With regards to high-affinity ligands, although they enable accurate determination of their entropic and stoichiometry contributions, the derivation of K_a is problematic owing to the steepness of the binding isotherm. In this case, displacement titrations could prove helpful in determining the complete thermodynamic signature [53,54]. Finally, entropic-driven ligands with a negligible enthalpic contribution make the thermodynamic analysis almost impractical; an illustrative example is the 3-hydroxy-3-methylglutaryl-CoA (HMG-CoA) reductase inhibitor fluvastatin [55].

Additional practical considerations need to be addressed when embarking on experimental ITC work. Both protein and ligand should reside in identical buffers to prevent large heats of dilution masking the true enthalpy. The solubility of both binding partners
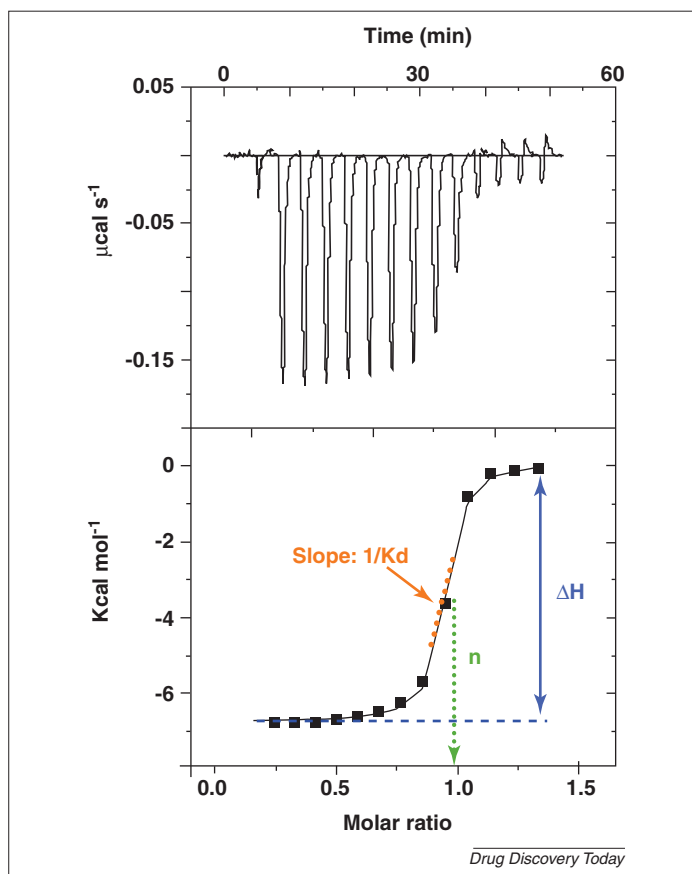
FIGURE 4

Raw data captured by a typical isothermal titration calorimetry (ITC) experiment **(a)**. The differential power is a function of time as the equilibrium of binding needs to set in after each consecutive titration step. The time integral of the peak therefore yields a measurement of thermal energy (ΔH) accompanied by each injection. The heat released or absorbed is in direct proportion to the amount of binding that occurs. When the protein in the cell becomes saturated with added ligand, the differential power signal diminishes until only the background heat of dilution is observed. The latter needs to be subtracted before accurate thermal analysis can be performed. To extract the different thermodynamic parameters, the heat formation is plotted against the molar ratio of ligand/protein **(b)**. By using data fitting for the suitable binding model, the change in enthalpy ΔH, the stoichiometry n, and the association constant K_a can be determined directly. The change in enthalpy corresponds to the intercept of the two asymptotic lines corresponding to the minimal and maximal heat formation, n controls the position of the inflection point, and the slope at the inflection point reflects the association constant ($K_a = 1/K_d$). The terms ΔS and ΔG are subsequently derived from these data.
Adapted from [49].

should be sufficiently high, keeping in mind that the concentration of the ligand is generally 15–20 times higher than the protein concentration.

A closer look at the enthalpic/entropic terms

Two major terms contribute to the entropy of binding, first, the desolvation entropy change and, second, the conformational entropy change. The desolvation entropy is favorable and originates from the release of water molecules as the ligand and the binding cavity undergo binding-driven desolvation. Favorable desolvation entropy is often the predominant force associated with the binding energy of hydrophobic groups. The desolvation event destroys the

organized water network around the ligand, resulting in a significant entropic gain [56,57]. A prevalent chemical design strategy is to add hydrophobic functionalities to an initial lead skeleton to attain more favorable entropy. By contrast, the conformational entropy change is usually unfavorable because the binding event entails the conformational rearrangement of the ligand and the target [40]. As such, molecular recognition of the ligand by the target limits the external rotational and translational freedom of both partners, leading to a conformational entropy penalty. In practice, this conformational entropy loss can be minimized through chemical constraints that make the unbound conformation of the ligand similar to its bioactive conformation. A widespread medicinal chemistry effort is to rigidify the skeleton to attain more favorable entropy. This could be achieved by the introduction of either a covalent bond or an intramolecular hydrogen bond. Apart from pre-organization, an added benefit of the latter might be that the enthalpic desolvation penalty of additionally populated extended conformations is partly compensated by the enthalpic gain of the intramolecular hydrogen bond upon binding. Because the main cause of entropy loss originates from structuring regions of the protein adjacent to the bound ligand, newly formed bonds should be aimed at pre-existing structured protein regions [58]. During lead optimization, the entropic term tends to increase; a recent ITC analysis of 250 target–ligand interactions revealed that, on average, synthetic agents present a greater favorable entropic contribution compared with biological ligands [59]. This is likely to reflect the ease with which medicinal chemists can manipulate the entropy term during lead optimization.

Although less pronounced in optimized compounds, enthalpic contributions are very familiar to medicinal chemists. They are in fact often the focus of structure–activity relationships during the iterative process of ligand optimization. However, the optimization of this parameter is very difficult even in the presence of X-ray crystallographic data [60], as described below.

There are two major contributors to the binding enthalpy. The first involves factors related to the formation of noncovalent interactions, such as intra- and intermolecular hydrogen bonds and van der Waals contacts. Whereas the former are always favorable, the latter can also be unfavorable (clashes and non-complementary interactions). The second major contributor involves the unfavorable factors, which are governed by the desolvation of polar moieties. Discrete noncovalent interactions are based on hydrogen bonds and/or electrostatic interactions. A favorable enthalpic term indicates that the target–drug complex engages in an intricate interaction network that upholds the unfavorable desolvation enthalpy. The enthalpy penalty associated with the desolvation of polar groups is in the order of 8 kcal mol^{-1}, about one order of magnitude higher than that of nonpolar groups [61]. In essence, the enthalpy provides the intrinsic signature of the forces that control the specific binding mode of a compound to its target. Medicinal chemists often observe that unfavorable enthalpies arise from ill-positioned polar groups in the compound [62–64]. Thus, merely adding hydrophilic moieties hoping to establish polar interactions can considerably reduce the overall enthalpy. It is not the number of polar groups present in the ligand that matters, but the quality of the newly formed noncovalent interactions. In this respect, several computational techniques have been applied to optimize the binding enthalpy

(specificity) by optimizing the electrostatic charge complementarity between the target and the drug [65,66]. The reason why lead optimization is characterized by an increased entropy contribution now becomes evident: the chemical design of a net positive number of polar bonds between a protein and a lead compound is exceptionally complex. Importantly, Freire *et al.* demonstrated the lack of correlation between the binding thermodynamic parameters (ΔH, ΔS) and Lipinski's rule of five [67].

An improvement in the binding enthalpy does not necessarily produce a higher binding affinity. The enthalpy–entropy compensation phenomenon implies that enthalpy gain can often be masked by entropy loss, resulting in a negligible enhancement of binding affinity. An enthalpic gain can be compensated by three main entropic factors: first, the loss of conformational freedom of highly flexible ligands; second, the structuring of protein regions by newly formed noncovalent interactions, resulting in a loss in conformational entropy; and third, the overexposure of hydrophobic groups, resulting in a loss in solvation entropy [68,69].

Entropic or enthalpic-dominant binding profile?

Compounds exhibiting comparable target binding affinities might have disparate enthalpic/entropic profiles. By resolving their energetic endowment, a differentiation among otherwise indistinguishable compounds can be made to steer compound prioritization and optimization. The question is: which thermodynamic profile has the greatest likelihood of displaying both high potency and off-target selectivity? To this end, it has been recently postulated that enthalpy-driven ligands are more selective, and achieve much higher binding affinities than do their entropically driven analogs [70]. This shows that comparative thermodynamic analysis of lead candidates could help identify enthalpically favored starting points. To illustrate this thesis, several examples are presented below that show the relevance of enthalpy and enthalpy contributions for various MoAs.

HIV-1 protease inhibition

Examination of the evolution of FDA-approved human immunodeficiency virus 1 (HIV-1) protease inhibitors indicated a trend towards enthalpy-driven agents. This profile is responsible for their high efficacy and low propensity to adaptability owing to mutations associated with drug resistance, and low toxicity [38,71–73].

HMG-CoA reductase inhibition

Statins, for which complete thermodynamic information has been published, suggest that a best-in-class compound entering the clinical setting is enthalpically better optimized than the original

first-in-class compound. It appears that the molecular interactions reflected in a better binding enthalpy are crucial for the development of improved ligands. It seems that compounds with extremely high affinity, good selectivity and superior drug resistance profiles are those with favorable binding enthalpies [55,74,75].

The individual thermodynamic variables have often been neglected as guiding tools in drug development because of experimental challenges. However, recent developments in instrumentation allow for the rapid and inexpensive derivation of thermodynamic parameters, which are then incorporated into optimization strategies. In other words, measuring enthalpic and entropic terms can provide priceless information for decision making in drug discovery.

Interpreting thermodynamic and kinetic data: lessons learnt

Test case: D-amino acid oxidase

A recent comparative study of six D-amino acid oxidase inhibitors has shed some light on how the thermodynamic and kinetic signatures of leads can be used to explain their MoA and select optimal tool compounds (Fig. 5) [76]. Both signatures were generated for all inhibitors. The derived K_d values found a good congruence with inhibition constants derived from a biochemical assay. Here, we describe a thorough kinetic and thermodynamic analysis for this system.

Thermodynamic signature

A mixture of enthalpic- and entropic-driven profiles were observed (Fig. 6). The rigid nature of the six inhibitors suggests low overall conformational entropy loss for the ligands. With respect to the target, *in silico* docking studies and X-ray analysis suggest a minimal loss of receptor conformational freedom upon binding. These data imply a negligible conformation entropy loss. By contrast, the desolvation entropic contribution is always favorable. These observations are in concurrence with the observed positive entropic contribution to the binding energy for all inhibitors.

Distinct differences in the thermodynamic signatures of the chemically related inhibitors 3 and 4 were observed, which differed by a single atom. Molecular dynamics simulations implied that interactions with water in the binding site were at the root of their dissimilar thermodynamic endowment. Inhibitor 3 displayed a richer hydrogen bond interaction network with active site waters, which reflects its higher enthalpic contribution. Conversely, the preservation of the structured water-network in the binding pocket upon binding implies opposing receptor conformational and desolvation entropy contributions, which results in
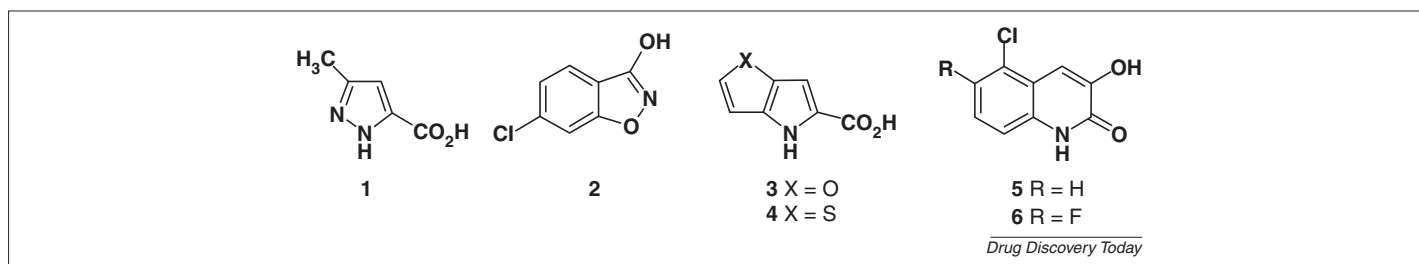

FIGURE 5

Chemical structures of the studied human D-amino acid oxidase (DAAO) inhibitors [76].
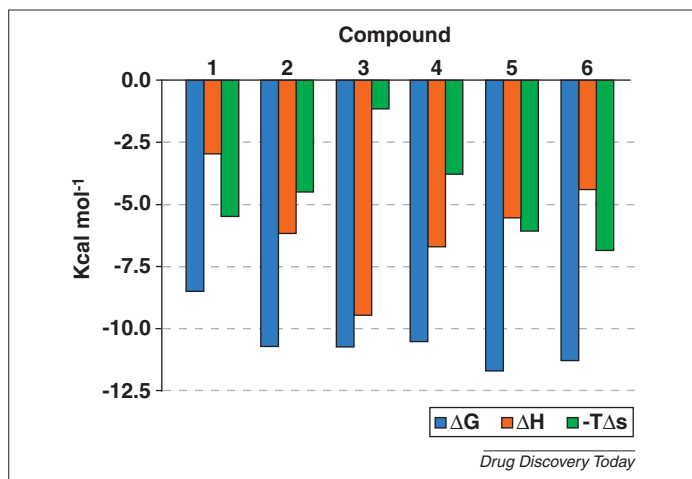
FIGURE 6

Thermodynamic profile of the binding of six human D-amino acid oxidase (DAAO) inhibitors based on isothermal titration calorimetry (ITC) measurements. The measured parameters include the Gibbs free energy of binding (ΔG), the enthalpy change (ΔH) and the temperature dependent entropy change ($-T\Delta S$).

inhibitor 3 having a lower entropic term than inhibitor 4. Inhibitors 3 and 4 are thus an elegant example of the enthalpy/entropy compensation phenomenon. A lesson learnt from this test case is that for this enzyme, the susceptibility of the inhibitors to interact with active site water molecules should be acknowledged and integrated in the optimization strategies.

Unlike inhibitors 3 and 4, inhibitors 5 and 6 did behave in line with the expectations. Their thermodynamic signatures were akin

in accordance with their similar physicochemical properties, such as log D, solubility and number of rotational bonds.

Kinetic signatures

A range of k_{on} and k_{off} constants were observed for the six inhibitors, which were all within the ordinary values observed for other biological systems (Fig. 7). As observed for other target–drug interaction complexes, the association rate constants demonstrated a modest deviation in magnitude (16-fold). This was expected because the diffusion rates of the different inhibitors are probably similar, given their similar physicochemical properties. By contrast, dissociation rates varied largely (1000-fold), giving rise to distinct K_d values. Interestingly, no dependency between k_{off} values and their respective enthalpy terms was found, which is in disagreement with observations by Tummino et al. that longer residence times are a direct consequence of enhancing the enthalpic contributions of protein–ligand interactions [5].

To establish the preferred kinetic profile, it was recommended that several inhibitors with a wide range of residence times should be followed up in vivo, which might give clues to the best kinetic profile that leads to maximal in vivo efficacy with minimal off-target side effects.

Intriguingly, a much lower association rate constant was measured for inhibitor 1. This finding was rationalized by the presence of two tautomers of inhibitor 1 in solution, where the less energetically favored one binds to the receptor. Upon binding of the sparsely populated active tautomer of inhibitor 1, the equilibrium is 'slowly' restored through an energy-costly isomerization reaction. An important lesson learnt from this system is that the occurrence of ligand tautomers in the solution phase must be
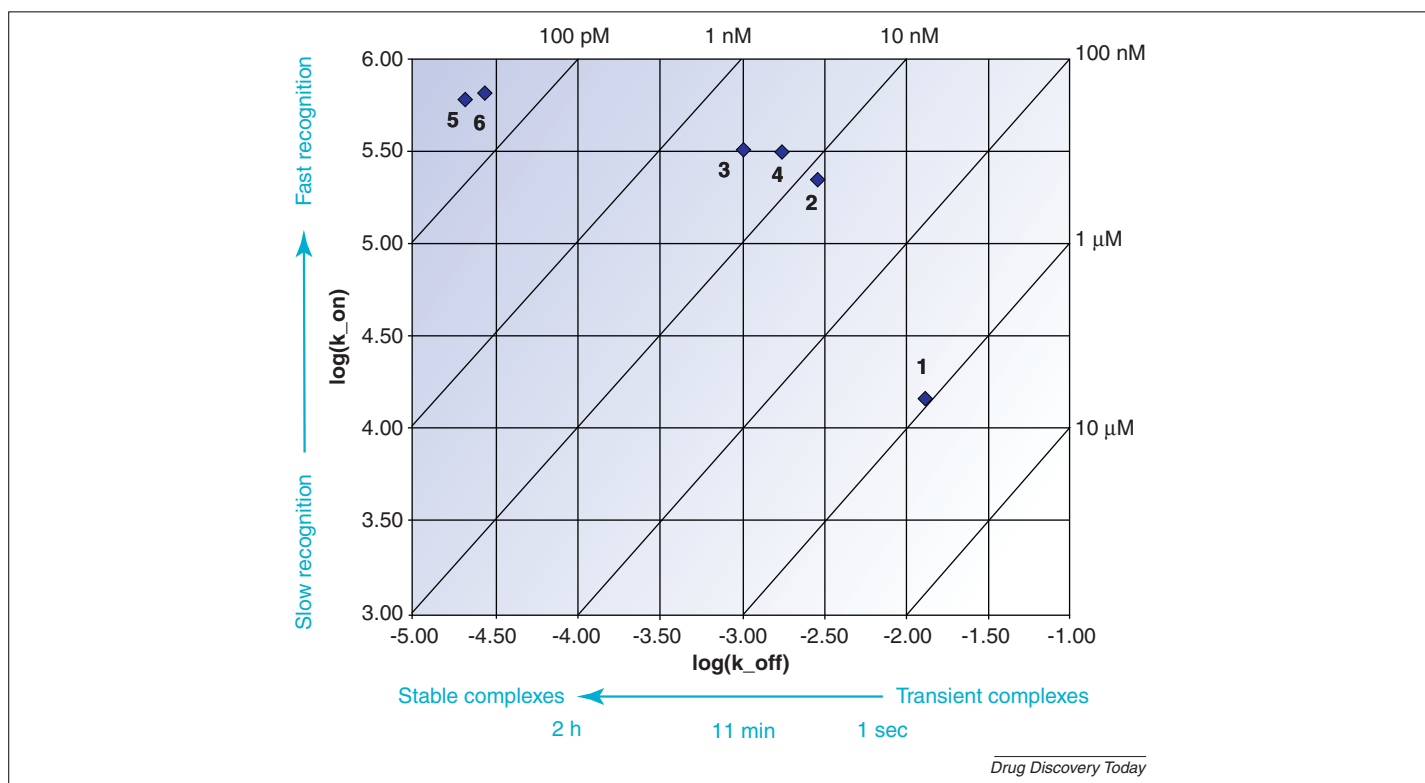

FIGURE 7

Second-order rate constant k_{on} plotted versus first-order-rate constant k_{off} of D-amino acid oxidase (DAAO) inhibitors 1–6 based on surface plasmon resonance measurements. The diagonal lines represent equal dissociation constant (K_d) levels.
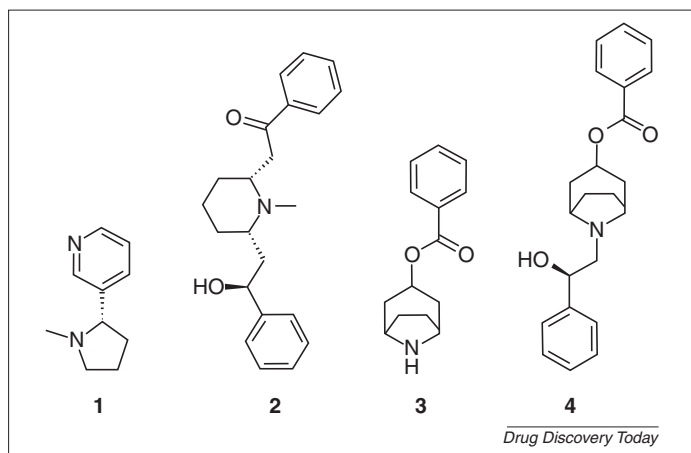
FIGURE 8

Chemical structures of the four *Aplysia californica* acetylcholine binding protein (Ac-AChBP) ligands studied [77].

FIGURE 9

Thermodynamic profile of the binding of four *Aplysia californica* acetylcholine binding protein (Ac-AChBP) ligands based on isothermal titration calorimetry (ITC) experiments. The measured parameters include the Gibbs free energy of binding (ΔG), the enthalpy change (ΔH) and the temperature dependent entropy change ($-T\Delta S$).

thoroughly investigated, and energetically demanding isomerization reactions circumvented.

Test case: acetylcholine binding protein

A recent comparative study of four *Aplysia californica* acetylcholine binding protein (Ac-AChBP) ligands has shed some light on how the thermodynamic signature can be used to elucidate the MoA of leads and guide chemical design (Fig. 8). The thermodynamic signature was generated for four ligands [77].

A mixture of enthalpic- and entropic-driven profiles was observed, the ligands ranging from very rigid to highly flexible. The rigid nature of nicotine (inhibitor 1) suggests a low or negligible conformational entropy loss from the ligand. Moreover, ligand binding is accompanied by conformational changes at the ligand-binding site [78], where the C-loop undergoes a large movement leading to a contraction of the amino acids surrounding the ligand. This rearrangement fixes the protein in a conformation optimal for interaction with the ligand, thus leading to a significant protein conformational entropy loss. By contrast, the desolvation entropy contribution of ligand binding is anticipated to be favorable but not enough to counterbalance the conformational entropy loss. The thermodynamic signature of inhibitor 1 is enthalpy driven, which is in full agreement with nicotine residing within a high ligand efficiency (LE) hotspot [79] (Fig. 9). Ligand binding is characterized by a close packing of a substantial number of aromatic and hydrophobic contributions, as well as close contacts between protein oxygens and the basic nitrogen of nicotine.

With regards to lobeline (inhibitor 2), the crystal structure of apo Ac-AChBP reveals an open loop-C. Structure-based evidence of Ac-AChBP in complex with lobeline shows that loop-C significantly changes conformation and wraps around lobeline forming specific interactions [80]. This suggests a certain degree of ligand and protein conformational entropy loss. Moreover, the desolvation entropy contribution of ligand binding is anticipated to be favorable and nearly counterbalances the unfavorable conformational entropy contribution. By contrast, the well-anchored lobeline in the binding site indicates a favorable enthalpic contribution.

VUF10663 (inhibitor 3) demonstrated entropic-driven behavior. Its enthalpic contribution is lower than that of inhibitor 1
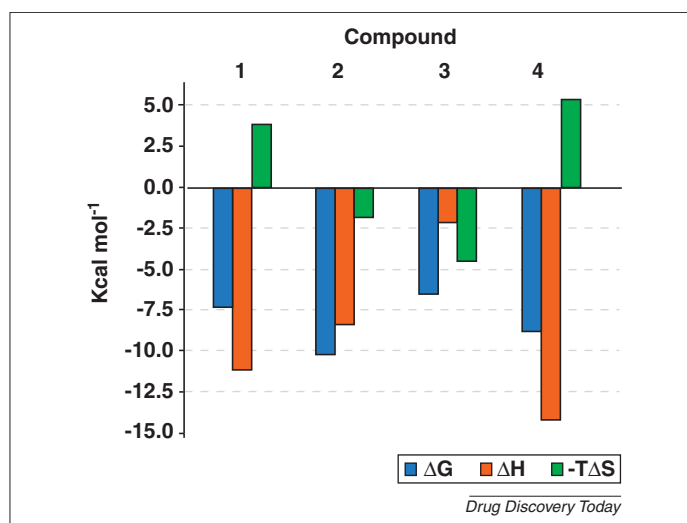
and inhibitor 2 because it does not present specific target–drug interactions in the binding site.

Next, the authors [77] attempted to merge inhibitor 2 and inhibitor 3 to design a hybrid with both high enthalpy and entropy contributions to the binding free energy. The result of this exercise, inhibitor 4 (VUF11437), showed an extremely favorable enthalpy contribution, but to the surprise of the authors, a rather opposing entropic behavior. In fact, the authors had predicted the entropic term to be as modest as those observed for inhibitor 2 and inhibitor 3. A plausible explanation proposed by the authors, and based on the crystal structure of Ac-AChBP in complex with inhibitor 4, is that inhibitor 4 is more rigidly fixed in the active site, provoking a lower flexibility of the protein (completely locked). This agrees with the high enthalpic contribution of inhibitor 4. It is another illustration of the enthalpy–entropy compensation phenomenon. A fragment optimization strategy proposed by the authors was allowing the protein a higher degree of flexibility while attempting to maintain the high target–drug interaction specificity.

Concluding remarks

We have summarized the evidence in favor of integrating thermodynamic and kinetic-based approaches for rational lead prioritization and optimization. Stated differently, the elucidation of the mode of ligand binding from the thermodynamic and kinetic signatures provides significant leverage in the identification of clinical candidates with optimal *in vivo* efficacy devoid of off-target or mechanism-based adverse events. Finally, we present a summary of the main TLI considerations outlined in this review.

- The triage and progression of chemical leads based primarily on their steady-state metrics has become obsolete.
- Understanding the binding mechanisms at the atomic level provides significant leverage in ligand optimization.
- The thermodynamic and kinetic signatures, in combination with structural biology and *in silico* modeling, help elucidate the driving mechanisms of target–drug binding.

- Enthalpy-driven compounds tend to present more potent and selective binding and efficacy profiles than do entropy-driven analogs.

- Residence time preference is highly dependent on the MoA and relevant pharmacological context. Longer k_{off} values are advised in those cases where mechanism-based toxicity is not a liability.

- Kinetic interrogation of the MoA with pharmacological tools spanning a range of residence times should be initiated as early as the target validation stage and maintained throughout all discovery phases.

- A k_{off} selectivity window is advisable to avoid off-target adverse events.

Acknowledgements

References

1 Swinney, D.C. (2004) Biochemical mechanisms of drug action: what does it take for success? *Nat. Rev. Drug Discov.* 3, 801–808

2 Kola, I. and Landis, J. (2004) Can the pharmaceutical industry reduce attrition rates? *Nat. Rev. Drug Discov.* 3, 711–715

3 Copeland, R.A. *et al.* (2006) Drug–target residence time and its implications for lead optimization. *Nat. Rev. Drug Discov.* 5, 730–739

4 Swinney, D.C. (2009) The role of binding kinetics in therapeutically useful drug action. *Curr. Opin. Drug Discov. Dev.* 12, 31–39

5 Tummino, P.J. and Copeland, R.A. (2008) Residence time of receptor–ligand complexes and its effect on biological function. *Biochemistry* 47, 5481–5492

6 Vauquelin, G. and Charlton, S.J. (2010) Long-lasting target binding and rebinding as mechanisms to prolong in vivo drug action. *Br. J. Pharmacol.* 161, 488–508

7 Lu, H. and Tonge, P.J. (2010) Drug–target residence time: critical information for lead optimization. *Curr. Opin. Chem. Biol.* 14, 467–474

8 Zhang, R. and Monsma, F. (2009) The importance of drug–target residence time. *Curr. Opin. Drug Discov. Dev.* 12, 488–496

9 Lu, H. *et al.* (2009) Slow-onset inhibition of the FabI enoyl reductase from *Francisella tularensis*: residence time and *in vivo* activity. *ACS Chem. Biol.* 4, 221–231

10 Rich, R.L. and Myszka, D.G. (2010) Grading the commercial optical biosensor literature-Class of 2008: 'The Mighty Binders'. *J. Mol. Recognit.* 23, 1–64

11 De Mol, N.J. and Fischer, M.J.E. (2010) Surface plasmon resonance: a general introduction. *Methods Mol. Biol.* 627, 1–14

12 Rich, R.L. and Myszka, D.G. (2006) Survey of the year 2006 commercial optical biosensor literature. *J. Mol. Recognit.* 20, 300–366

13 Geitmann, M. *et al.* (2010) Interaction kinetic and structural dynamic analysis of ligand binding to acetylcholine-binding protein. *Biochemistry* 49, 8143–8154

14 Schuck, P. and Zhao, H. (2010) The role of mass transport limitation and surface heterogeneity in the biophysical characterization of macromolecular binding processes by SPR. *Methods Mol. Biol.* 627, 15–54

15 Markgren, P.O. *et al.* (2002) Relationships between structure and interaction kinetics for HIV-1 protease inhibitors. *J. Med. Chem.* 45, 5430–5439

16 Magotti, P. *et al.* (2009) Structure–kinetic relationship analysis of the therapeutic complement inhibitor compstatin. *J. Mol. Recognit.* 22, 495–505

17 Vauquelin, G. (2010) Rebinding: or why drugs may act longer *in vivo* than expected from their *in vitro* target residence time. *Expert Opin. Drug Discov.* 5, 927–941

18 Kumar, P. *et al.* (2009) Update of KDBI: Kinetic Data of Bio-molecular Interaction database. *Nucleic Acids Res.* 27, D636–D641

19 Hanahan, D. and Weinberg, R.A. (2000) The hallmarks of cancer. *Cell* 100, 57–70

20 Copeland, R.A. (2005) Evaluation of enzyme inhibitors in drug discovery. A guide for medicinal chemists and pharmacologists. *Methods Biochem. Anal.* 46, 1–265

21 Erhlich, P. (1913) Chemotherapeutics: scientific principles, methods and results. *Lancet* 2, 445–451

22 Shaikh, S.A. *et al.* (2007) From drug target to leads – sketching a physicochemical pathway for lead molecule design *in silico*. *Curr. Pharm. Des.* 13, 3454–3470

23 Vauquelin, G. and Van Liefde, I. (2006) Slow antagonist dissociation and long-lasting *in vivo* receptor protection. *Trends Pharmacol. Sci.* 27, 356–359

24 Lipton, S.A. (2006) Paradigm shift in neuroprotection by NMDA receptor blockade: memantine and beyond. *Nat. Rev. Drug Discov.* 5, 160–170

25 Kapur, S. and Seeman, P. (2000) Antipsychotic agents differ in how fast they come off the dopamine D2 receptors. Implications for atypical antipsychotic action. *J. Psychiatry Neurosci.* 25, 161–166

26 Kapur, S. and Seeman, P. (2001) Does fast dissociation from the dopamine D_2 receptor explain the action of atypical antipsychotics?: a new hypothesis. *Am. J. Psychiatry* 158, 360–369

27 Swinney, D.C. (2006) Can binding kinetics translate to a clinically differentiated drug? From theory to practice. *Lett. Drug Des. Discov.* 3, 569–574

28 Mousa, S.A. *et al.* (2001) Platelet GPIIb/IIIa binding characteristics of small molecule RGD mimetic: distinct binding profile for Roxifiban. *Br. J. Pharmacol.* 13, 331–336

29 Van Liefde, I. and Vauquelin, G. (2009) Sartan-AT1 receptor interactions: in vitro evidence for insurmountable antagonism and inverse agonism. *Mol. Cell. Endocr.* 30, 237–243

30 Lewandowicz, A. *et al.* (2003) Achieving the ultimate physiological goal in transition state analogue inhibitors for purine nucleoside phosphorylase. *J. Biol. Chem.* 278, 31465–31468

31 Vanderheyden, P.M. *et al.* (2000) Angiotensin II type 1 receptor antagonists. Why do some of them produce insurmountable inhibition? *Biochem. Pharmacol.* 60, 1557–1563

32 Fuchs, B. *et al.* (2000) Comparative pharmacodynamics and pharmacokinetics of candesartan and losartan in man. *J. Pharm. Pharmacol.* 52, 1075–1783

33 Vincent, J.P. and Lazdunski, M. (1973) The interaction between α-chymotrypsin and pancreatic trypsin inhibitor (Kunitz inhibitor). Kinetic and thermodynamic properties. *Eur. J. Biochem.* 38, 365–372

34 Dierynck, I. *et al.* (2007) Binding kinetics of darunavir to human immunodeficiency virus type 1 protease explain the potent antiviral activity and high genetic barrier. *J. Virol.* 81, 13845–13851

35 King, N.M. *et al.* (2004) Structural and thermodynamic basis for the binding of TMC114, a next-generation human immunodeficiency virus type 1 protease inhibitor. *J. Virol.* 78, 12012–12021

36 VanCott, T.C. *et al.* (1994) Dissociation rate of antibody-gp120 binding interactions is predictive of V3-mediated neutralization of HIV-1. *J. Immunol.* 153, 449–459

37 Wood, E.R. *et al.* (2004) A unique structure for epidermal growth factor receptor bound to GW572016 (Lapatinib): relationships among protein conformation, inhibitor off-rate, and receptor activity in tumor cells. *Cancer Res.* 64, 6652–6659

38 Ohtaka, H. and Freire, E. (2005) Adaptive inhibitors of the HIV-1 protease. *Prog. Biophys. Mol. Biol.* 88, 193–208

39 Ruben, A.J. *et al.* (2006) Overcoming roadblocks in lead optimization: a thermodynamic perspective. *Chem. Biol. Drug Des.* 67, 2–4

40 Chaires, J.B. (2008) Calorimetry and thermodynamics in drug design. *Ann. Rev. Biophys.* 37, 135–151

41 Velázquez-Campoy, A. *et al.* (2001) The binding energetics of first- and second-generation HIV-1 protease inhibitors: implications for drug design. *Arch. Biochim. Biophys.* 390, 169–175

42 Cornish-Bowden, A. (2002) Enthalpy–entropy compensation: a phantom phenomenon. *J. Biosci.* 27, 121–126

43 Silverstein, K.A.T. *et al.* (2001) Hydrophobicity in a simple model of water: entropy penalty as a sum of competing terms via full, angular expansion. *J. Chem. Phys.* 114, 6303–6314

44 Li, Z. and Lazaridis, T. (2003) Thermodynamic contributions of the ordered water molecule in HIV-1 protease. *J. Am. Chem. Soc.* 125, 6636–6637

45 Young, T. *et al.* (2007) Motifs for molecular recognition exploiting hydrophobic enclosure in protein–ligand binding. *PNAS* 104, 808–813

46 Beuming, T. *et al.* (2009) High-energy water sites determine peptide binding affinity and specificity of PDZ domains. *Protein Sci.* 18, 1609–1619

47 Pearlstein, R.A. *et al.* (2010) New hypotheses about the structure–function of proprotein convertase subtilisin/kexin type 9: analysis of the epidermal growth factor-like repeat A docking site using WaterMap. *Proteins* 78, 2571–2586

48 Ladbury, J.E. *et al.* (2010) Adding calorimetric data to decision making in lead discovery: a hot tip. *Nat. Rev. Drug. Discov.* 9, 23–27

49 Holdgate, G.A. and Ward, W.H. (2005) Measurements of binding dynamics in drug discovery. *Drug Discov. Today* 10, 1543–1550

50 Turnbull, W.B. and Daranas, A.H. (2003) On the value of c: can low affinity systems be studied by isothermal titration calorimetry? *J. Am. Chem. Soc.* 125, 14859–14866

51 Myszka, D.G. *et al.* (2003) The ABRF-MIRG'02 study: assembly state, thermodynamic, and kinetic analysis of an enzyme/inhibitor interaction. *J. Biomol. Tech.* 14, 247–269

52 Ciulli, A. *et al.* (2006) Probing hot spots at protein–ligand binding sites: a fragment-based approach using biophysical methods. *J. Med. Chem.* 49, 4992–5000

53 Velázquez-Campoy, A. and Freire, E. (2005) ITC in the post-genomic era? Priceless. *Biophys. Chem.* 115, 115–124

54 Velázquez Campoy, A. and Freire, E. (2006) Isothermal titration calorimetry to determine association constants for high-affinity ligands. *Nat. Protoc.* 1, 186–191

55 Carbonell, T. and Freire, E. (2005) Binding thermodynamics of statins to HMG-CoA reductase. *Biochemistry* 44, 11741–11748

56 Tanford, C. (1980) *The hydrophobic effect: formation of micelles and biological membranes*. John Wiley and Sons

57 Homans, S.W. *et al.* (2007) Water, water everywhere – except where it matters? *Drug Discov. Today* 12, 534–539

58 Freire, E. (2009) A thermodynamic approach to the affinity optimization of drug candidates. *Chem. Biol. Drug Des.* 74, 468–472

59 Olsson, T.S. *et al.* (2008) The thermodynamics of protein–ligand interaction and solvation: insights for ligand design. *J. Mol. Biol.* 384, 1002–1017

60 Davis, A.M. *et al.* (2003) Application and limitations of X-ray crystallographic data in structure-based ligand and drug design. *Angew. Chem. Int. Ed. Engl.* 42, 2718–2736

61 Cabani, S. *et al.* (1981) Group contributions to the thermodynamic properties of non-ionic organic solutes in dilute aqueous solution. *J. Solut. Chem.* 10, 563–595

62 Robertson, A.D. and Murphy, K.P. (1997) Protein structure and the energetics of protein stability. *Chem. Rev.* 97, 1251–1267

63 Hilser, V.J. *et al.* (1996) The enthalpy change in protein folding and binding: refinement of parameters for structure-based calculations. *Proteins* 26, 123–133

64 Ladbury, J.E. (2007) Enthalpic efficiency and the role of thermodynamic data in drug development: possibility or a pipeline dream! *Eur. Pharmaceut. Rev.* 12, 59–62

65 Altman, M.D. *et al.* (2008) Computational design and experimental study of tighter binding peptides to an inactivated mutant of HIV-1 protease. *Proteins* 70, 678–694

66 Sherman, W. and Tidor, B. (2008) Novel method for probing the specificity binding profile of ligands: applications to HIV protease. *Chem. Biol. Drug Des.* 71, 387–407

67 Lipinski, C.A. *et al.* (1997) Experimental and computational approaches to estimate solubility and permeability in drug discovery and development settings. *Adv. Drug Deliv. Rev.* 46, 3–26

68 Freire, E. (2008) Do enthalpy and entropy distinguish first in class from best in class? *Drug Discov. Today* 13, 869–874

69 Lafont, V. *et al.* (2007) Compensating enthalpic and entropic changes hinder binding affinity optimization. *Chem. Biol. Drug Des.* 69, 413–422

70 Freire, E. (2004) Isothermal titration calorimetry: controlling binding forces in lead optimization. *Drug Discov. Today: Technol.* 1, 295–299

71 Ohtaka, H. *et al.* (2004) Thermodynamic rules for the design of high affinity HIV-1 protease inhibitors with adaptability to mutations and high selectivity towards unwanted targets. *Int. J. Biochem. Cell. Biol.* 36, 1787–1799

72 Ohtaka, H. *et al.* (2003) Multidrug resistance to HIV-1 protease inhibition requires cooperative coupling between distal mutations. *Biochemistry* 42, 13659–13666

73 Ohtaka, H. *et al.* (2002) Overcoming drug resistance in HIV-1 chemotherapy: the binding thermodynamics of Amprenavir and TMC-126 to wild-type and drug-resistant mutants of the HIV-1 protease. *Prot. Sci.* 11, 1908–1916

74 Sarver, R.W. *et al.* (2008) Thermodynamic and structure guided design of statin based inhibitors of 3-hydroxy-3-methylglutaryl coenzyme A reductase. *J. Med. Chem.* 51, 3804–3813

75 Park, W.K. *et al.* (2008) Hepatoselectivity of statins: design and synthesis of 4-sulfamoyl pyrroles as HMG-CoA reductase inhibitors. *Bioorg. Med. Chem. Lett.* 18, 1151–1156

76 Lange, J.H.M. *et al. Eur. J. Med. Chem.*, doi:10.1016/j.ejmech.2011.04.023, in press

77 Edink, E. *et al.* (2011) Fragment growing induces conformational changes in acetylcholine-binding protein: a structural and thermodynamic analysis. *JACS* 133, 5363–5371

78 Celie, P.H.N. *et al.* (2004) Nicotine and carbamylcholine binding to nicotinic acetylcholine receptors as studied in AChBP crystal structures. *Neuron* 41, 907–914

79 De Kloe, G.E. *et al.* (2010) Surface plasmon resonance biosensor based fragment screening using acetylcholine binding protein identifies ligand efficiency hot spots by deconstruction of nicotinic acetylcholine receptor α7 ligands. *J. Med. Chem.* 53, 7192–7201

80 Hansen, S.B. *et al.* (2005) Structures of Aplysia AChBP complexes with nicotinic agonists and antagonists reveal distinctive binding interfaces and conformations. *EMBO J.* 24, 3635–3646